Desalination 492 (2020) 114496

Contents lists available at ScienceDirect

Desalination

journal homepage: www.elsevier.com/locate/desal

Development of AgCl-TiO_2 xerogels entrapped antibacterial polyacrylonitrile membranes: The effect of high salinity water on silver release, antibiofouling and antibacterial efficacies

Metin Uz[a,b], Filiz Yasar Mahlicli[a], Erol Seker[a], Sacide Alsoy Altinkaya[a,*]

[a] Izmir Institute of Technology, Department of Chemical Engineering, Gulbahce Campus, Urla, Izmir 35430, Turkey
[b] Iowa State University, Department of Chemical and Biological Engineering, 2114 Sweeney Hall, Ames, IA 50011, United States of America

GRAPHICAL ABSTRACT

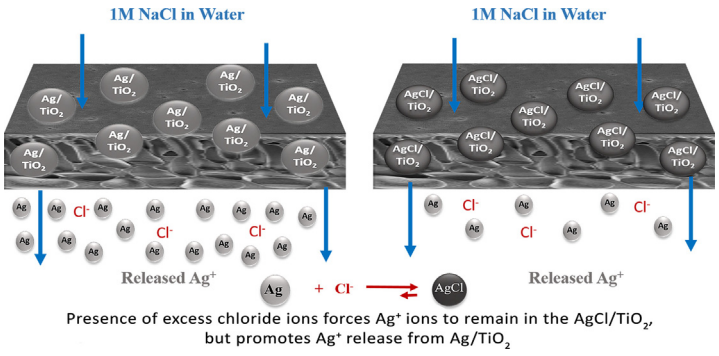

ARTICLE INFO

Keywords:
Antibacterial ultrafiltration membrane
Silver xerogel
Antifouling
Water treatment
Sustained silver release

ABSTRACT

Silver-containing antibacterial membranes are commonly used to control biofouling during bacteria filtration. Unfortunately, fast and uncontrolled release of silver to water is a challenge since this causes mass accumulation of silver in water resources and insufficient long-term antimicrobial effect. To overcome these disadvantages, we propose to add AgCl-TiO_2 xerogels (0–0.8 wt%) in the polyacrylonitrile membranes. The long-term silver retaining of the membranes was evaluated by measuring the silver release under filtration of deionized water in the absence and the presence of 1 M NaCl up to 5 days. The antibiofouling and the antibacterial efficacies were determined by measuring the changes in antibacterial activity and DI water flux of the membranes at the end of 5 days of *E. coli* filtration. The 0.2 wt% AgCl-TiO_2 xerogel incorporated polyacrylonitrile membrane demonstrated a constant ~1 μg of silver release/cm^2 per filtration cycle after a total filtration of 0.05 L/cm^2 with 1 M NaCl solution. Additionally, it showed antibacterial efficacy and ~100% recovery of deionized water flux by simple backwashing with water after having been used in many *E. coli* filtration cycles. Thus, this membrane could potentially be used up to ~5.8 years for 8000 h a year for the filtration of high salinity water.

Statement of novelty: Silver-containing antibacterial membranes are commonly used to control biofouling during bacteria filtration. Uncontrolled release of silver from the membrane causes massive silver accumulation in water which in turn leads to contamination of water resources and threat to aquatic organisms. Although silver release is strongly influenced by the salinity of water, the release data was collected through filtration of pure DI water or tap water in literature. To overcome the shortcomings of the published studies, we propose to use AgCl-

* Corresponding author.
E-mail addresses: metinuz@iyte.edu.tr, metinuz@iastate.edu (M. Uz), filizyasar@iyte.edu.tr (F. Yasar Mahlicli), erolseker@iyte.edu.tr (E. Seker), sacidealsoy@iyte.edu.tr (S. Alsoy Altinkaya).

https://doi.org/10.1016/j.desal.2020.114496
Received 24 January 2020; Received in revised form 23 April 2020; Accepted 28 April 2020
Available online 23 June 2020
0011-9164/

TiO_2 xerogels in membranes due to low solubility of AgCl in water and measure the release by filtering high-salinity water.

1. Introduction

According to the recent report of World Health Organization (WHO, 2019) [1], it is estimated that in the following years, diarrhea will still kill around 1 million people annually mostly children under the age of 5 as a result of unsafe drinking water. Diarrhea linked to water is mainly caused by pathogenic microorganisms; thus, microbial control in water is extremely important to prevent outbreaks of waterborne diseases. Microbial safety is also an important issue in wastewater treatment plants. Chemical disinfectants such as chlorine, chloramines and ozone are commonly used to inactivate microorganisms. However, these agents react with various constituents in water causing the formation of harmful, carcinogenic disinfection byproducts (DBPs) [2]. Furthermore, some pathogens develop resistance to chemical disinfectants and this requires extremely high disinfectant dosage. More recently, several natural and engineered antimicrobial nanomaterials including chitosan [3], silver nanoparticles (nAg) [4], photocatalytic TiO_2 [5,6], fullerol [7], aqueous fullerene nanoparticles (nC60) [8], and carbon nanotubes (CNT) [9] have been proposed to replace conventional disinfectants. Although the nanomaterials are not expected to produce harmful DBPs, there are three important challenges for large scale use of these nanomaterials in water treatment. The first challenge is the stability of nanoparticles in water. Commercial metal oxide nanoparticles, Fe_2O_3, ZnO, NiO, SiO_2, TiO_2, ZnO were found to aggregate quickly in water [10,11] and the most effective dispersion of the particles was achieved with ultrasonication [11]. The second challenge is the retention and recycle of nanoparticles for reuse in continuous treatment cycles. It is envisioned that the nanomaterials can be used for small decentralized water systems. Third challenge is associated with the threat to aquatic organisms such as crustaceans, algae and fish.

Membrane filtration is an advanced water treatment solution to produce bacteria- free water. However, biofouling caused by the deposition, growth and metabolism of bacterial cells or flocs on membranes is considered as a major problem. The biofouling causes not only lower sustainable flux but also more environmental footprint as a result of frequent membrane cleaning with harsh chemicals. Strong biocides, such as chlorine, ozone, hypochlorite, chlorinated phenolics, and non-oxidative biocides like quaternary ammonium salts with high concentrations are commonly used to avoid/eliminate biofilm formation [12]; however, this strategy can damage the membrane integrity, increase operational cost and produce large waste streams. To overcome these challenges, the membranes were functionalized with active antimicrobial nanoparticles, such as silver, titania or silver-exchanged zeolites [13]. Among these materials, silver nanoparticles have demonstrated significant antibacterial activity against numerous types of bacteria [14]; hence, they are utilized in developing silver-containing antibacterial membranes. Silver-containing antibacterial membranes were mostly prepared in thin film composite structure and silver nanoparticles were added during polymerization [15,16] or coating [17–33] of the selective layer. Incorporation of nanoparticles during interfacial condensation can adversely affect the polymer chemistry and properties of the selective layer. On the other hand, employing surface coating techniques requires charged or reactive groups on the surface and in the absence of these groups, the surface needs to be first functionalized through plasma [17,24,25] or wet chemistry [19,30]. Most of the polymers used in membrane manufacturing do not carry charged groups; hence, they require surface activation of the support membrane and then incorporate nanoparticles on the modified surface in a selective layer, which increases the cost of the membrane production. In addition, scale-up of surface modification and nanoparticle incorporation raises many challenges, such as the necessity of changes to current manufacturing processes, thus, rendering scale-up very difficult. In contrast, mixed matrix membranes, developed by dispersing silver nanoparticles in polymer matrixes [19,28,34–37], have the advantages of low cost, ease of fabrication and high density of nanoparticles achievable through the cross section of the membranes [38]. The critical challenge in the preparation of silver-containing mixed matrix membranes is to achieve the controlled release rate of silver which results in long-term antimicrobial effect and no mass accumulation of silver in water resources. In literature, only a few studies focused on controlling the release rate of silver ions from the membranes [19,24,39] and the release was usually followed over a short period of time [15,16,18,23,25,31,35,36]. Although silver release is strongly influenced by the salinity of water, the release data, published up until now, was collected through filtration of pure DI water or tap water that contained 0.05 M NaCl.

To overcome the shortcomings of the published studies, we propose to use AgCl-TiO_2 xerogels in polyacrylonitrile (PAN) membranes in this study. One may expect to have negligible silver release from AgCl-TiO_2 xerogels due to low solubility of AgCl in DI water and NaCl containing water. Thus, we claim that Ag could dissolve much more than AgCl in the presence of chloride ions, since there is initially no Ag in the membrane containing AgCl. Chloride ion in the solution does not react with AgCl in the membrane; in other words, chloride ion does not dissolve silver from AgCl nanoparticles. To prove our hypothesis, we prepared PAN membranes using both AgCl-TiO_2 and Ag-TiO_2 xerogels. The long-term silver retaining of these membranes were evaluated by measuring the silver release under filtration of DI water in the absence and the presence of 1 M NaCl up to 5 days. 1 M NaCl concentration was selected considering the average chloride concentrations in high salinity industrial wastewater streams, which changes between 35 and 70 g/L. [40] The antibiofouling and the antibacterial efficacies of the membranes were determined by measuring the changes in antibacterial activity and DI water flux at the end of 5 days of *E. coli* filtration. To the best of our knowledge, this is the first study proposing the use of AgCl-TiO_2 xerogels to control the silver release during water filtration in the presence of excess chloride ions. In fact, for the first time, we demonstrate the effect of an industrially relevant NaCl concentration (1 M) on silver release (in other words, silver retaining in membrane), antibacterial and antibiofouling efficacies of Ag and AgCl incorporated mixed matrix membranes.

2. Materials and methods

2.1. Materials

Polyacrylonitrile (PAN) with a molecular weight of 150 kDa, dimethyl sulfoxide (DMSO) and sodium chloride (NaCl) were purchased from Sigma Aldrich. Agar, Mueller Hinton Broth, Nutrient Broth and Peptone used for antibacterial tests were supplied by Sigma Aldrich. In the synthesis of silver chloride containing titania (AgCl-TiO_2) xerogels, silver nitrate (99% purity, from Sigma-Aldrich Co., USA) was used as a silver precursor. Tetrabutyl orthotitanate (TBOT) (99% purity, from Sigma-Aldrich Co., USA), nitric acid (65% purity, from Sigma-Aldrich Co., USA) and ethanol (99% purity, from Sigma-Aldrich Co., USA) were used without further purification. Reagent-grade deionized water (DI) was used in preparation of aqueous solutions (Arium 61316 water purification system, Sartorius). *Escherichia coli* strain (ATCC25922) used in all antibacterial tests was obtained from American Type Culture Collection (ATCC).

2.2. Methods

2.2.1. Preparation and characterization of Ag-TiO_2 and AgCl-TiO_2 xerogels

In this study, silver and silver chloride containing titania (Ag-TiO_2 and AgCl-TiO_2) xerogels with 29 wt% Ag and AgCl content were synthesized by using a silver nitrate precursor through the sol-gel process described in our previous works [39,41]. The synthesized xerogels were characterized using X-ray diffraction (XRD) to confirm the structure. Silver contents in Ag-TiO_2 and AgCl-TiO_2 xerogels were the same since in the preparation of AgCl-TiO_2 xerogel, we first synthesized Ag-TiO_2 xerogel and then this was followed by HCl acid treatment of this xerogel to convert Ag into AgCl [39,41].

2.2.2. Preparation of PAN membranes

The membranes were prepared using dry/wet phase inversion technique. Briefly, 1.2 g of PAN was dissolved in 10 mL of dimethyl sulfoxide (DMSO) at room temperature with continuous stirring. Following the PAN dissolution, the predetermined amounts of Ag-TiO_2 or AgCl-TiO_2 xerogels (0.08, 0.2 and 0.8 wt%) were incorporated into the casting solution. The solution was then cast on a glass support using an automatic film applicator (Sheen, Automatic film applicator-1133N, Kingston, England) at a speed of 100 mm/s. The wet thickness of the membranes was adjusted to 150 μm by using a four-sided applicator. Immediately after casting, the membranes were placed into an environmental chamber (Siemens, Simatic OP7, Massa Martana, Italy) and dried for 30 s at 25 °C and 40% relative humidity. Then, the films were immersed in a water bath at room temperature and incubated 24 h. The membranes prepared were coded as PAN- x% AgCl- TiO_2 or PAN- x% Ag-TiO_2 where AgCl-TiO_2 and Ag-TiO_2 indicate the type of xerogel and x% represent weight percentage of xerogel incorporated into the membranes. The composition of PAN in all membranes was fixed at 12 wt%.

2.2.3. Characterization of membranes

The morphology of the membrane surface and cross-section was examined using a scanning electron microscope (SEM) (FEI Quanta). For the cross-section imaging, the membranes were freeze-fractured under liquid nitrogen. Prior to SEM imaging, the membranes were sputter-coated with a gold layer. The surface hydrophobicity/hydrophilicity of the membranes was evaluated by measuring the contact angle in optical tensiometer (Theta Lite, Attension Instruments). A series of magnified pictures of the water droplets (~6 μL) on the top surfaces of all the membranes were obtained by the optic tensiometer at room temperature. Continuous images were recorded starting from the initial contact of water droplet with membrane surface until the droplet shape becomes stable. The measurements were taken from at least seven different locations on each membrane to determine the experimental uncertainty in the measurements. The mechanical testing was conducted by following the ASTM D882 tensile and elongation test standards. Briefly, membrane segments with 10 cm of length and 1 cm of width were placed in between the tensile tester grips. A crosshead speed range of 10 mm/min was applied with 30 kN grips using a universal testing machine (Instron).

Ultrafiltration experiments were carried out using a dead-end stirred-cell filtration system (Amicon Stirred Ultrafiltration Cell, Model 8050 UF, Millipore Corp) with a cell capacity of 50 mL and an active surface area of 13.4 cm^2. After inserting membrane, the cell was filled with 50 mL of DI water. Following the initial membrane compaction at 1.5 bar, the water flux was measured at 1 bar for each membrane by recording the amount of water filtered as a function of filtration time.

2.2.4. Long-term silver release from membranes

The long-term silver release from the membranes was determined under dynamic conditions. Briefly, the membranes were placed in the module and the cell was filled with either 50 mL of DI water or 50 mL of DI water with 1 M NaCl concentration. Following one-time compaction at 1.5 bar, the DI water (with or without 1 M NaCl) was filtered through the membranes at 1 bar for 3 times a day, i.e. constituting one cycle, during 5 days of filtration. At the end of each cycle, the membranes were kept in 50 mL of DI water or 50 mL of DI water with 1 M NaCl concentration under static conditions and the filtration was restarted next day. The filtered water samples (50 mL) were collected during the initial compaction, filtration and overnight storing in DI water or 1 M NaCl containing DI water at the end of each cycle in separate tubes during 5 days of filtration. The silver concentration in the permeate samples was quantified using a 7500ce Series inductively coupled plasma quadruple mass spectrometer (ICP-MS) (Tokyo, Japan) without further dilution. For the ICP-MS analysis, the collected samples in tubes were adjusted to contain 2% (w/v) nitric acid and filtered to remove any impurities before the analysis. Prior to analyses, the calibration curve was established using a silver standard. The used membranes were kept for further evaluation of their antibacterial activity.

2.2.5. Biofouling resistance of membranes

In many studies in the literature, *E. coli* bacteria were used to evaluate the biofouling resistance of the membranes; thus, we also used *E. coli* as a model microorganism in this study. *E. coli* was cultured on Mueller-Hinton agar at 37 °C to a mid-log phase. The bacteria colonies were collected with a swab from the agar plate and dispersed into 0.1 wt% peptone water until the McFarland value reached 0.5, which corresponds to 10^8 Colony Forming Units per milliliter (CFU/mL). The bacteria solution (10^8 CFU/mL) was then re-suspended in 1 mM phosphate buffer at pH 7.4 to obtain a feed solution with the bacterial density of 10^6 CFU/mL. To evaluate biofouling resistance of the membranes, first the DI water flux of the clean membranes at 1 bar was measured. Then, 187 L/m^2 of bacteria containing mixture (10^6 CFU/mL) (which corresponds to total volume of 250 mL bacteria solution) was filtered and at the end, the membranes were taken out, reversed and placed back into the dead-end filter for backwashing with 150 mL of DI water at 1 bar. Following the backwash, the membranes were reversed back again and the DI water flux was re-measured and the decline in flux caused by biofouling was calculated from the difference in water fluxes, measured before and after filtration using bacterial mixture. The membranes after backwashing and water filtration were dried, and several surface SEM images were taken (~20 images per membrane). By counting the number of bacteria per unit area using Image J analysis, the bactericidal ratio (%) was calculated by the following equation [42].

$$\text{Bacterial ratio (\%)} = \left(\frac{N_p - N_m}{N_p}\right) \times 100$$

where N_P and N_M are numbers of visual bacterial colonies counted on the pristine and AgCl/TiO_2 xerogel containing membranes, respectively. Before the SEM imaging, bacteria samples on the membrane surface were fixed with 4% paraformaldehyde for 10 min and washed with PBS buffer (1× pH 7.4) three times with 7 min waiting period in each wash. Then, gradual ethanol dehydration procedure was applied in the following order: 35% Ethanol (1 × 15 min), 50% Ethanol (1 × 15 min), 70% Ethanol (1 × 15 min), 80% Ethanol (1 × 15 min), 90% Ethanol (1 × 15 min), 95% Ethanol (2 × 15 min), 100% Ethanol (3 × 20 min). After this, the samples were immersed in 2 mL hexamethyldisilazane solution for 30 min and then left drying at room temperature. The dried samples were mounted, and sputter-coated with gold before the SEM analysis.

2.2.6. Antibacterial activity of membranes

A disk diffusion test which is a practical and quick approach was used in order to determine the antibacterial activity of the membranes [15,25,30]. The method is a qualitative visual test but it was already applied and found suitable for evaluating the antibacterial activity of AgCl/TiO_2 and Ag/TiO_2 xerogels used in this study [41]. In the disk

diffusion tests, *E. coli* was cultured (10^8 CFU/mL, as described in Section 2.2.5) and spread onto the Mueller-Hinton agar plate. Following the bacterial seeding, the fresh and used membranes (i.e. subjected to 5 cycles of 1 M NaCl filtration), sterilized by ultraviolet radiation for 15 min, were immediately placed in the middle of bacteria seeded agar plates and incubated for 24 h at 37 °C to determine if there was bacterial growth. At the end of the incubation, the diameter of clear zones around the membranes free from the bacteria was observed.

2.2.7. Statistical analysis

Throughout this study, significant differences between groups of experimental data were evaluated using ANOVA analysis by Tukey's method with 95% confidence interval. The results were presented as standard mean errors calculated from at least three independent experiments. In each of these experiments, three replicates were performed.

3. Results and discussion

3.1. Characterization of membranes

AgCl/TiO_2 and Ag/TiO_2 xerogels, used to prepare the xerogels containing PAN membranes, were synthesized in the same way as reported in our previous study [39]. Fig. 1 shows the XRD patterns of both 29 wt% AgCl/TiO_2 and 29 wt% Ag/TiO_2 xerogels which were analyzed using X'Pert HighScore Plus software and JCPDS-International Centre for Diffraction Data (ICDD) (Powder Diffraction File (PDF-2 Database)). As seen in the figure, the major diffraction peaks located at 25.3°, 37.8°, and 48.1° belong to anatase crystalline phase of TiO_2 while the major diffraction peaks observed at 27.9°, 32.3° and 46.2° correspond to diffraction peaks of AgCl crystalline phase in TiO_2. Ag crystalline phase in TiO_2 had the peaks located at 38.3°, 44.6°, and 64.7°.

We confirmed the presence of Ag/TiO_2 or AgCl/TiO_2 xerogels in the membranes and the chemical composition of these membranes by running an energy-dispersive X-ray spectroscopy (EDX) analysis. Fig. 2A–B show the distribution of silver on the membrane surface and in the cross section, respectively. An increase in the atomic percentage of Ti and Ag was observed with the increased xerogel loading, (Fig. 2C–E). The surface and cross section morphology of the unloaded and AgCl-TiO_2 xerogels loaded PAN membranes were characterized by SEM (shown in Fig. 3).

All of the membranes demonstrated finger-like pores in the bulk structure along with a thin dense skin layer on the surface of the membrane. During phase inversion, a polymer rich skin layer was formed due to the dragging of polymer molecules to the top surface via solvent evaporation, which simultaneously created polymer lean porous phase at the bottom of the membrane surface. The presence of AgCl-TiO_2 xerogels did not cause any change in the classical finger-like porous morphology of the unloaded PAN membranes regardless of the xerogel concentration. In addition, xerogel particle agglomeration was not observed either on the top and bottom surfaces or throughout the cross section, as seen in Fig. 3M–O. This could be attributed to the small crystallite sizes of Ag (< 5 nm) and AgCl (< 60 nm) stabilized by TiO_2 in the xerogels [41]. The SEM images were analyzed using Image J software to determine pore sizes on the surfaces, total and dense layer thicknesses as described before [43]. The results given in Table 1 showed that xerogel addition had no significant influence on the total or dense skin layer thicknesses of the membranes. Also, the difference in the pore size of the pristine and 0.08% xerogel containing membranes was found statistically insignificant ($p > 0.05$). On the other hand, when the xerogel content was increased to 0.2%, the surface pore size became larger ($p < 0.05$). This can be explained by the high specific area and hydrophilic nature of the xerogels. Both properties enhanced the penetration of water vapor into casting solution during evaporation and resulted in an instantaneous demixing in the coagulation bath, consequently, a more porous structure compared to the plain membrane. Adding 0.8 wt% xerogel made an opposite effect on the mass transfer during the evaporation step. Accumulation of xerogels close to the surface through evaporation and increased viscosity of casting solution slowed down the exchange of solvent and nonsolvent during coagulation and caused delayed precipitation which led to smaller sized pores on the surface [44,45]. A similar trend was also observed in the work of Li et al. [46]. The hydrophilicity of the membranes was significantly improved as confirmed by the decrease in the contact angle of bare PAN membrane from 70° to 45° through adding 0.8 wt% xerogel (Table 1). This can be explained by significant hydrophilic nature of the sol-gel made TiO_2 xerogels as reported in previous studies [47–49].

Atomic force microscopy (AFM) analyses results in Fig. 4 indicated that the difference between the roughness of the PAN and 0.08 wt% AgCl-TiO_2 xerogels containing PAN membranes are statistically insignificant ($p > 0.05$). On the other hand, increasing xerogel loading to 0.8 wt% in the membranes reduced the surface roughness, which in turn affected the antibiofouling performance of this membrane. The decrease in roughness could be ascribed to the reaction between the hydroxyl groups on the xerogels and nitrile group on the PAN through hydrogen bonding and the covalent bonding between silver and NH and C—N groups in PAN as suggested in another study [50,51].

The mechanical properties and pressure stability of the membranes were also tested. The tensile test results represented in Fig. 5A indicated that the tensile strength, elongation at break (%), and Young's modulus values of the plain membrane did not change through xerogel addition. This is an expected result since the xerogel content in the membranes is very low compared to the loading levels used in other studies. For instance, Li et al. [46], reported an increase in the tensile strength of the polyethersulfone (PES) membrane from 3.21 MPa to 4.07 MPa while a decrease in the elongation ratio from 15.62% to 11.37% but they added 5 wt% TiO_2 into the casting solution. The stability of the membranes was tested at 3 bar and no defects were observed either visually or under the microscope as shown by the SEM pictures in Fig. 5B through E for the pristine and 0.2 wt% AgCl/TiO_2 xerogel loaded membranes. The filtration pressure could not be increased above 3 bar since the recommended operating pressure for the dead-end filtration module was 3 bar. Because the membranes prepared in this study are in the

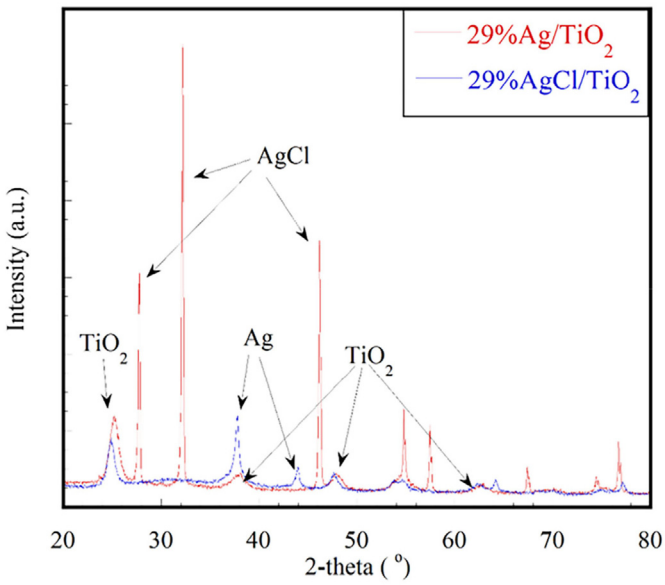

Fig. 1. XRD patterns of 29%Ag/TiO_2 and 29%AgCl/TiO_2. Diffraction peaks for Ag, AgCl and TiO_2 indicated on the figure were determined using JCPDS-International Centre for Diffraction Data (ICDD), Powder Diffraction File (PDF-2 Database), Newtown Square, Pennsylvania (2000). Reproduced with permission from Ref. [39]. Copyright 2015 Elsevier.

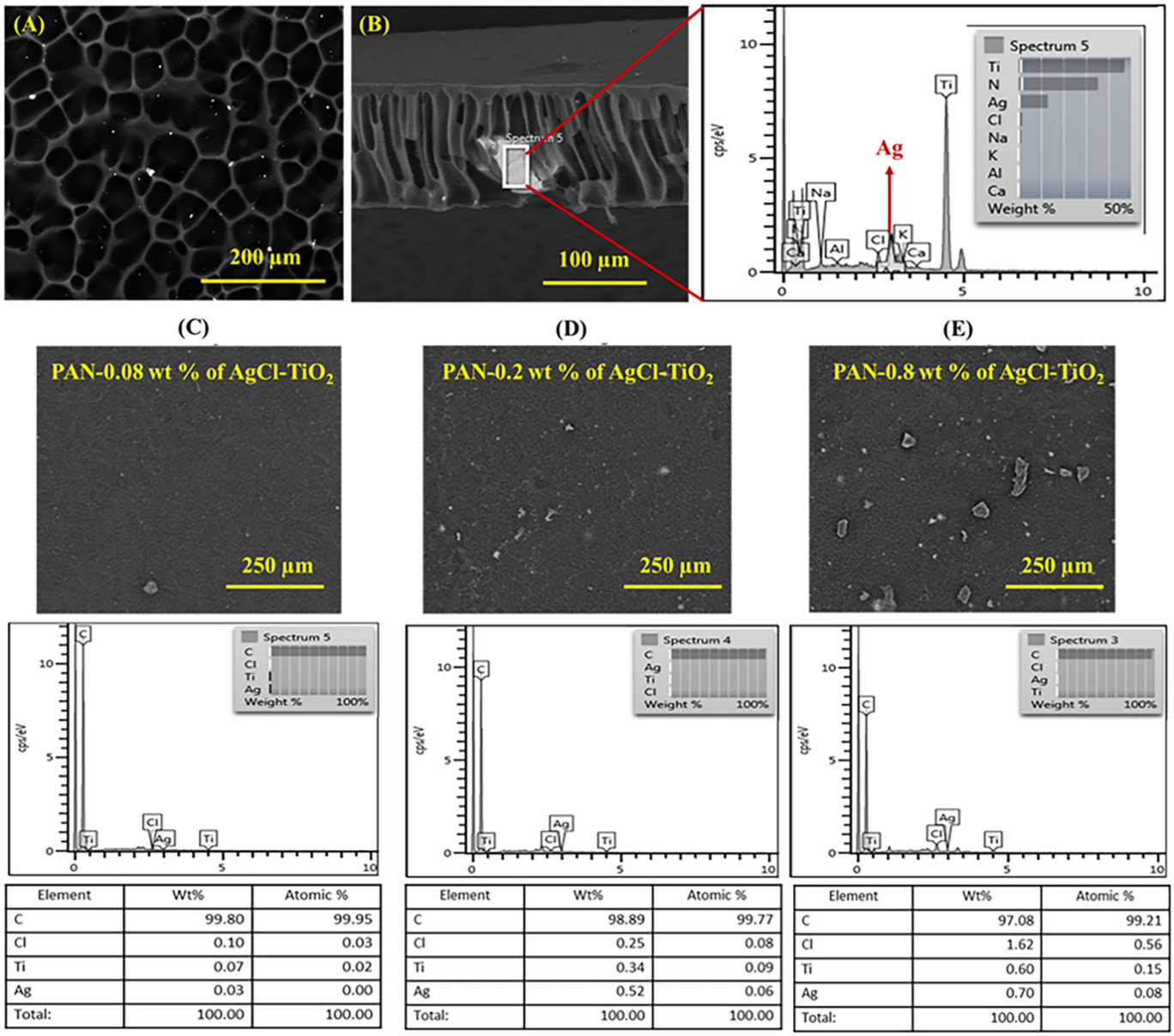

Element	Wt%	Atomic %
C	99.80	99.95
Cl	0.10	0.03
Ti	0.07	0.02
Ag	0.03	0.00
Total:	100.00	100.00

Element	Wt%	Atomic %
C	98.89	99.77
Cl	0.25	0.08
Ti	0.34	0.09
Ag	0.52	0.06
Total:	100.00	100.00

Element	Wt%	Atomic %
C	97.08	99.21
Cl	1.62	0.56
Ti	0.60	0.15
Ag	0.70	0.08
Total:	100.00	100.00

Fig. 2. (A) SEM back scattering images and (B) EDX scanning of AgCl-TiO_2 xerogels within the PAN-0.8 wt% of AgCl-TiO_2 membrane cross-section. EDX scanning of AgCl-TiO_2 xerogels on the surfaces of (C) PAN-0.08 wt% of AgCl-TiO_2 (D) PAN-0.2 wt% of AgCl-TiO_2 (E) PAN-0.8 wt% of AgCl-TiO_2 membranes.

ultrafiltration (UF) category and UF process is typically operated in the pressure range of 1–5 bar, the pressure resistance of the membranes was found sufficient.

Fig. 6 shows the pure water permeability values of the bare and mixed matrix membranes which have been found to be in the range of typical ultrafiltration membranes [52]. Upon loading 0.2 wt% of AgCl-TiO_2 xerogel in the matrix, the pure water permeability of the bare PAN membrane was enhanced from ~200 L/m^2 h bar to 400 L/m^2 h bar as a consequence of larger pore sizes and a more hydrophilic surface. Increasing xerogel content from 0.2 wt% to 0.8 wt% resulted in a significant decrease in the permeability down to ~250 L/m^2 h bar (Fig. 6). This result indicated that the pore size rather than hydrophilicity was the controlling parameter for the water permeability. This conclusion was reached since the most hydrophilic surface was obtained with 0.8 wt% xerogel loading while the largest pore size was detected on 0.2 wt% xerogel loaded PAN membrane (Table 1). The water flux of the membranes after 3 days of long-incubation in the water bath did not change suggesting that the polymer chain and membrane structure were not altered due to the sorption of water.

3.2. Release studies

Silver-containing membranes have received considerable attention since they have been shown to prevent biofouling by controlling the growth of pathogenic microorganisms and their spoilage. It was demonstrated that the antimicrobial activity of the silver nanoparticles (AgNPs) was solely due to Ag^+ release and most importantly, a concentration as low as 15 µg/L of Ag^+ was effective against *E. coli* bacteria [53]. Thus, the controlled release of the silver ions from the membrane to the aqueous environment is critical to obtain the desired concentrations necessary for preventing biofilm formation. High release rates cause the accumulation of silver in the environment and also fast depletion of silver from the membrane, which shortens the life of the membrane. To the best of our knowledge, most studies have shown that silver nanoparticles (AgNPs) incorporated membranes are prone to uncontrollable silver release and a few studies have shown that this release increases further in the presence of NaCl in aqueous solutions [54]. We postulate that instead of AgNPs, the use of AgCl nanoparticles (AgCl-NPs) could lower silver release in the presence of NaCl. This is

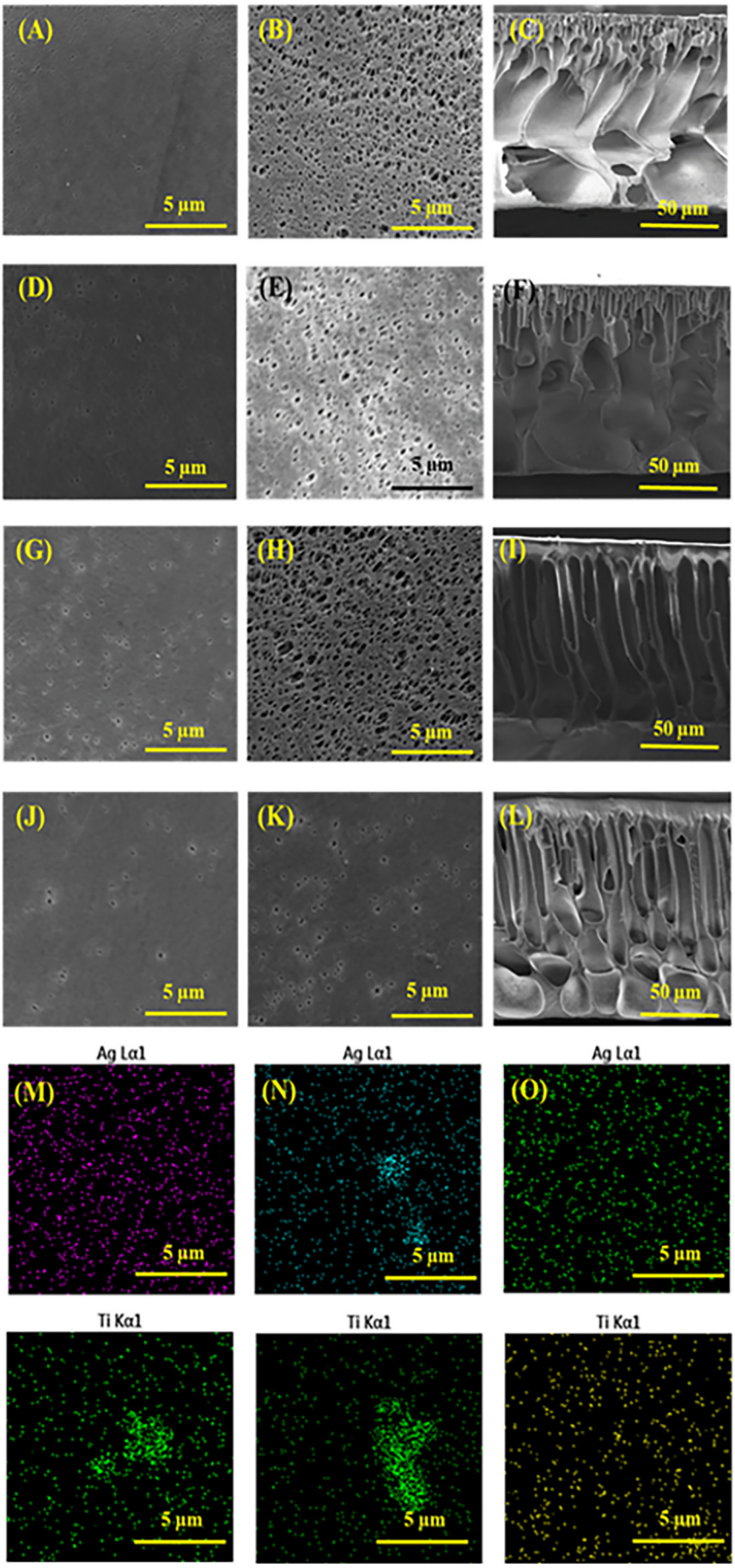

(caption on next page)

Fig. 3. Surface and cross-section SEM images of the membranes. PAN control membranes (A) dense surface (top of the membrane) (B) porous surface (bottom of the membrane) (C) cross-section. PAN-0.08 wt% of AgCl-TiO_2 (D) dense surface (E) porous surface (F) cross-section. PAN-0.2 wt% of AgCl-TiO_2 (G) dense surface (H) porous surface (I) cross-section. PAN-0.8 wt% of AgCl-TiO_2 (J) dense surface (K) porous surface (L) cross-section. Surface images: 20000× magnification. Cross-section images: 2000× magnification. EDX mapping of membranes (M) PAN-0.08 wt% of AgCl-TiO_2 (N) PAN-0.2 wt% of AgCl-TiO_2 (O) PAN-0.8 wt% of AgCl-TiO_2.

because the equilibrium solubility product constants for dissolution of AgCl are much lower than that of Ag. At 25 °C, the equilibrium constants for the $[AgCl_2]^-$, $[AgCl_2]^{-2}$ and $[AgCl_2]^{-3}$ complex formation reactions shown in Eqs. (2)–(4) are 4.47×10^{-5} L/mol, 7.59×10^{-5} L^2/mol^2, 3.02×10^{-5} L^3/mol^3, respectively while for metallic silver in Cl^- containing water to form $AgCl_{(aq)}$ is very high, $> 10^3$ mol/L [54–56]

$$AgCl_{(s)} \rightleftharpoons Ag^+_{(aq)} + Cl^-_{(aq)} \quad (1)$$

$$AgCl_{(s)} + Cl^-_{(aq)} \rightleftharpoons AgCl^-_{2(aq)} \quad (2)$$

$$AgCl_{(s)} + 2Cl^-_{(aq)} \rightleftharpoons AgCl^{2-}_{3(aq)} \quad (3)$$

$$AgCl_{(s)} + 3Cl^-_{(aq)} \rightleftharpoons AgCl^{3-}_{4(aq)} \quad (4)$$

To prove our hypothesis of low solubility of AgCl-NPs as compared to AgNPs in NaCl containing water, the amount of silver leached out from the AgCl-TiO_2 and Ag-TiO_2 incorporated PAN membranes was measured during the filtration of both DI water and DI water containing 1 M NaCl. Fig. 7 shows the silver release (μg/cm^2) from each membrane as a function of total volume filtered (L/m^2).

The silver loss from AgCl-TiO_2 containing PAN membranes was found to be less than that from Ag-TiO_2 containing PAN membranes during filtration of both DI and NaCl containing DI water. This finding is consistent with the dissolution chemistry given in Eqs. (1)–(4). In the presence of 1 M NaCl, the silver losses from the membranes containing 0.08%, 0.2% and 0.8% Ag-TiO_2 xerogels were 4.7 and 3.6 times higher than the losses from the corresponding membranes loaded with AgCl-TiO_2.xerogels This in fact proves our hypothesis that instead of using Ag-TiO_2 xerogel in membranes, AgCl-TiO_2 usage resulted in much lower silver loss even in the presence of excess Cl^- ions in water with 1 M NaCl concentration. One may expect lower silver release during filtration of NaCl containing water since the presence of Cl^- ions must force the reaction (Eq. (1)) in reverse to decrease the solubility of AgCl. However, our results showed that the presence of NaCl slightly increased the solubility of AgCl due to the formation of silver complexes. The results in Fig. 8A and B clearly indicate that using DI water for testing for the long-term stability of silver-containing membranes leads to misleading results.

For all the PAN membranes incorporated with AgCl-TiO_2 xerogels, after an initial fast silver release, a plateau was reached during filtration of 1 M NaCl solution (Fig. 7A–C). The initial fast silver release was mainly controlled by mass transfer while in the plateau region the chemical reaction equilibrium, shown in Eqs. (1)–(4), controlled the release rate. In contrast, there was no plateau observed when water was filtered, which indicated that the dissolution chemical reaction equilibria were not reached. In addition, NaCl filtration, that caused the deposition of AgCl on the Ag-TiO_2 containing PAN membranes complicated the dissolution behavior of silver nanoparticles. The amount of silver loss increased with the increased xerogel content for both NaCl solution and DI water filtration (Fig. 7A–F). A stepwise increase in the release was observed, particularly at high Ag-TiO_2 contents (0.2 and 0.8 wt%), during the 1 M NaCl filtration (Fig. 7D–F). This stepwise increase was due to the silver release which occurred during overnight treatment of all the membranes in water and 1 M NaCl containing water without stirring the contents [57]. Enhanced dissolution and release of Ag^+ ion from the silver nanoparticles in the presence of excess Cl^- ions was also reported in the work of Levard et al. [54], and was in parallel with our findings.

Our calculations indicated that regardless of xerogel loading, 9.85 wt% of the initial silver loading was lost from the PAN membranes containing AgCl-TiO_2 xerogel at the end of 5 days of 1 M NaCl filtration whereas silver loss from the PAN membranes containing 0.2 wt% and 0.8 wt% Ag-TiO_2 xerogel was 36.1 wt% (Fig. 8A). Previous studies in literature measured the release of silver nanoparticles using DI water or a very low concentration of Cl^- ions which did not represent the actual conditions found in the industrial applications [19,23,30,35,36]. For instance, Dankovich et al. [58], reported 132 μg/L of silver release from the silver nanoparticles in paper films, corresponding to 3.4 wt% Ag loss per liter, using 5.9 g/L NaCl as test solution while the silver loss was 105 μg/L in the case of DI water usage. These results were reported based on the total of 1 L of DI water or 5.9 g/L NaCl filtration for one cycle and also no time for the release was specified. The NaCl concentration (5.9 g/L) used in this study was ~10 times smaller than 1 M NaCl concentration (58.44 g/L) used in our study and it was much lower than the typical values measured in wastewater streams [40]. To mimic the harsh NaCl environment in high salinity wastewater streams or in seawater, we utilized 1 M NaCl solution for filtration studies. Our results demonstrated that using AgCl rather than Ag within a xerogel matrix decreased silver release rate and also increased long-term use in the presence of excess chlorine ions.

3.3. Anti-biofouling tests

The anti-biofouling property of the membranes was tested through the filtration of *E. coli* solution (total of 187 L/m^2 *E. coli* solution filtered). At the end of the bacterial filtration, the number of bacteria on the membrane surface was determined using SEM and the water fluxes were remeasured after backwashing with water. We utilized anti-adhesion and antimicrobial approaches to impart biofouling resistance to the membranes. We attempted to increase hydrophilic nature and reduce the roughness of the membranes through xerogel addition to

Table 1
Morphological properties and contact angle values of AgCl-TiO_2 incorporated PAN membranes. (a, b, and * $p < 0.05$).

Xerogel Content in PAN Membranes (wt %)	Surface Pore Size on the Dense Side (μm)	Surface Pore Size on the Porous Side (μm)	Dense-skin Layer Thickness (μm)	Total Thickness (μm)	Contact Angle (°)
0	0.10 ±0.08	0.42 ±0.16	12.0 ±0.7	103.0 ±1.1	70.0 ±2.8*
0.08	0.20 ±0.04	0.40 ±0.12	11.0 ±0.4	102.3 ±0.4	57.5 ±1.4*
0.2	**0.30 ±0.06[a]**	**0.69 ±0.09[b]**	10.8 ±1.0	102.7 ±1.2	49.8 ±0.3*
0.8	**0.11 ±0.05[a]**	**0.25 ±0.06[b]**	12.1 ±1.6	101.3 ±1.0	45.0 ±0.7*

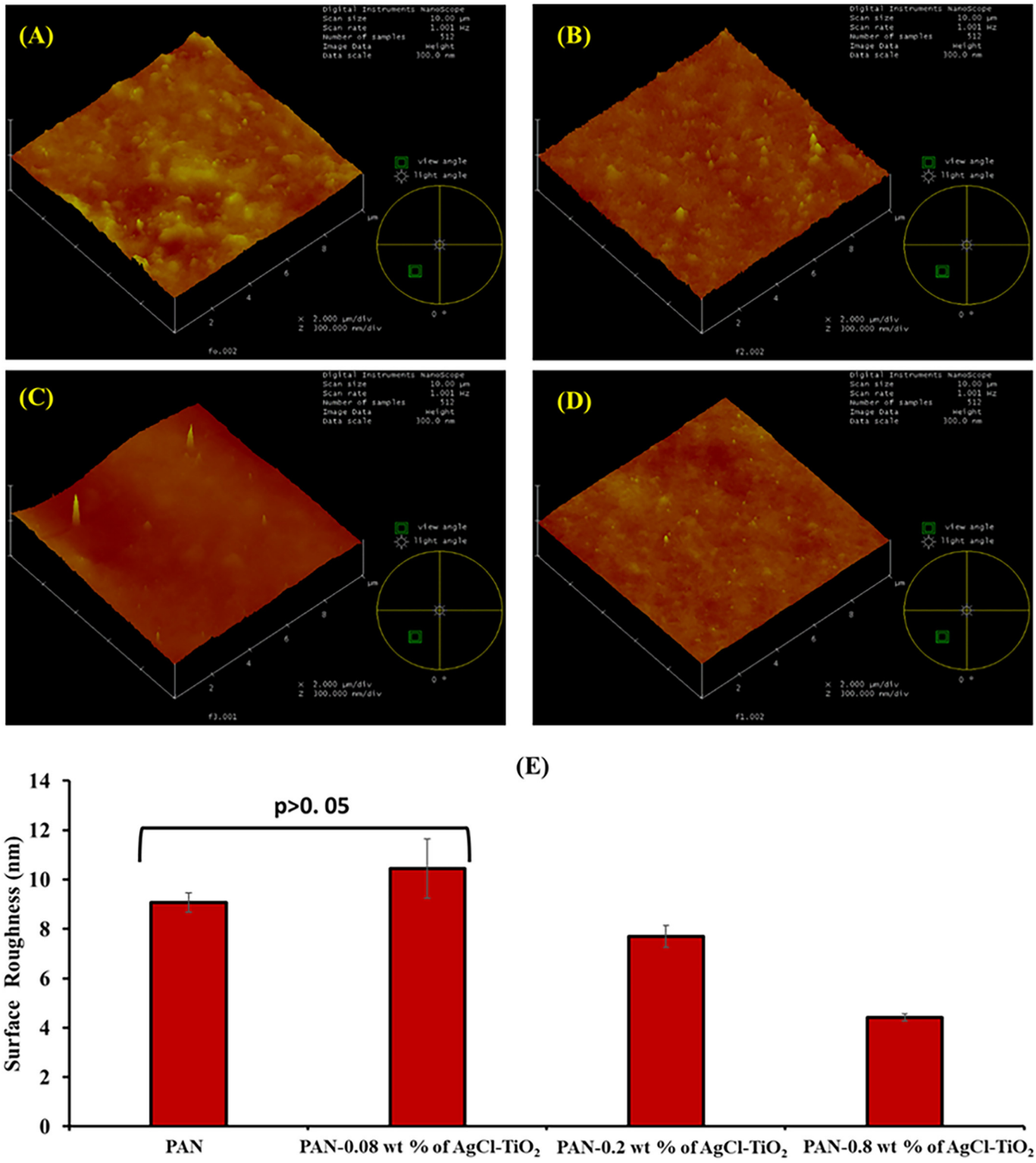

Fig. 4. AFM surface roughness images of membranes (A) PAN (B) PAN-0.08 wt% of AgCl-TiO_2 (C) PAN-0.2 wt% of AgCl-TiO_2 (D) PAN-0.8 wt% of AgCl-TiO_2. (E) Surface roughness values of membranes.

decrease initial adsorption or attachment of bacteria. These efforts aim to prevent the accumulation of bacteria in the valleys of rough surfaces [59] and attachment of *E coli* on hydrophobic surfaces [60]. Fig. 9 shows that the least number of bacteria accumulated on the 0.8 wt% xerogel loaded PAN membrane which has the most smooth and hydrophilic surface among all the membranes prepared.

This result simply confirmed that the xerogel addition improved the anti-adhesion properties of the PAN membrane. The 0.2 and 0.8 wt% xerogel containing membranes showed almost 100% water flux recoveries after bacteria filtration (Fig. 10) although 0.8 wt% xerogel addition resulted in a more anti-adhesive surface. This observation can be explained by similar antibacterial activities of these two membranes as shown in Fig. 11. The results in Figs. 9 through 11 allowed concluding that controlling the surface roughness and hydrophilicity

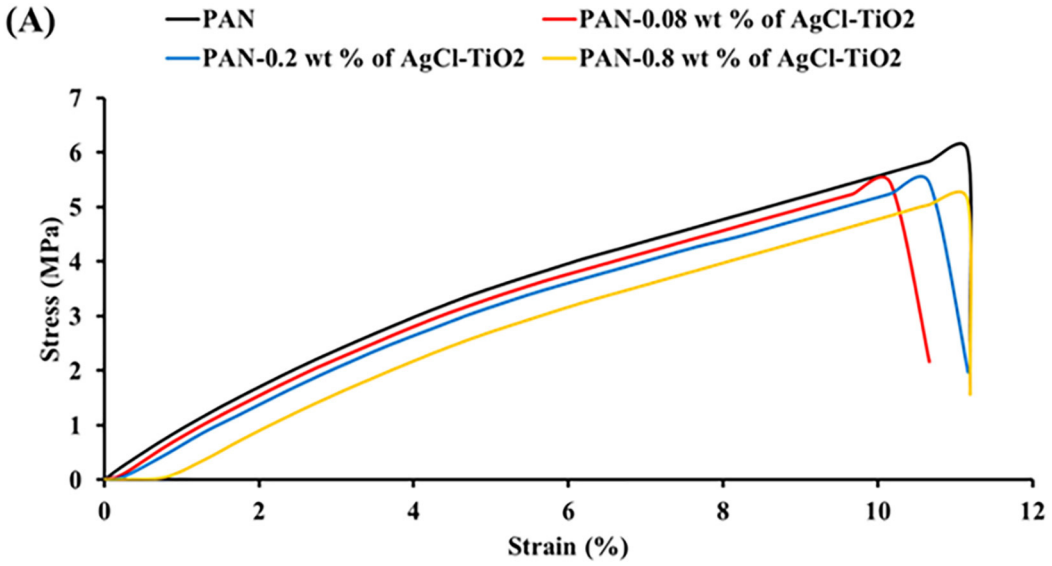

Xerogel Content in PAN Membranes (wt. %)	Tensile Strength (MPa)	Elongation at Break (%)	Young's Modulus (MPa)
0	6.04 ±1.3	11.21 ±0.55	44.53 ±2.1
0.08	5.44 ±1.1	10.66 ±0.47	43.98 ±3.4
0.2	5.43 ±0.76	11.16 ±1.5	43.24 ±1.5
0.8	5.13 ±0.98	11.20 ±1.3	44.52 ±4.3

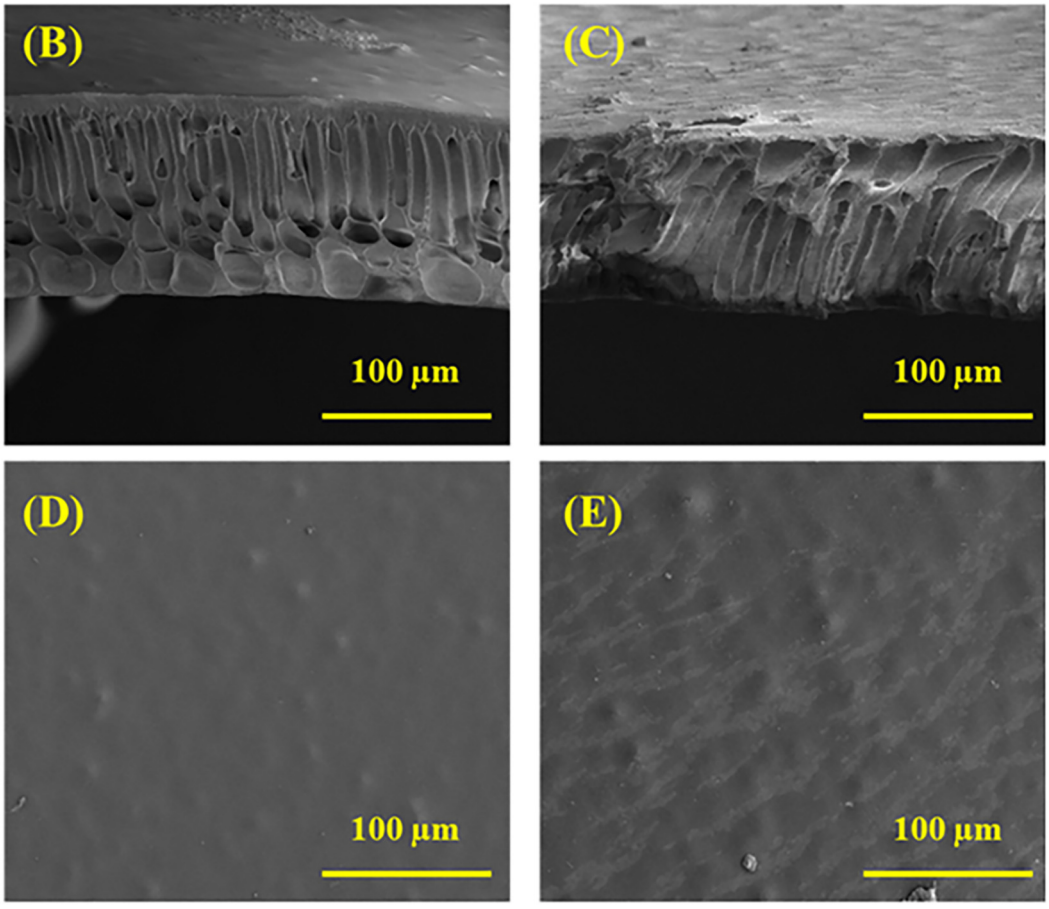

Fig. 5. (A) Stress and strain plot for PAN and xerogel incorporated PAN membranes. Cross section SEM images of (B) PAN (C) 0.2% AgCl-TiO_2 xerogels containing PAN membranes. Surface SEM images of (D) PAN (E) 0.2% AgCl-TiO_2 xerogels containing PAN membranes taken after being exposed to 3 bar pressure resistance

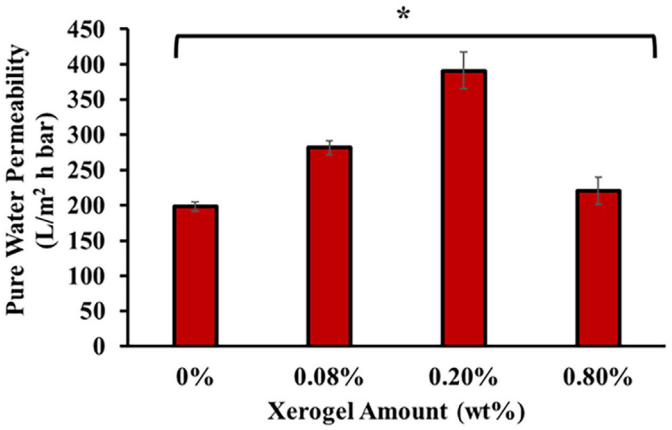

Fig. 6. Pure water permeability of AgCl-TiO_2 xerogel incorporated PAN membranes. *Represent the statistically significant difference (* $p < 0.05$).

prevented the early bacteria attachment and biofilm formation. On the other hand, the antibacterial activity of the surfaces provided additional protection for an extended period through killing or suppressing the activity of bacteria before they attached to the surface. Thus, the combined action of antibiofouling and antibacterial efficacy of our membranes prevented the accumulation of *E coli* on the surface resulting in total flux recovery after bacteria filtration when the xerogel loading levels were 0.2 and 0.8 wt%. 0.08 wt% xerogel loading was not sufficient to impart fully antibacterial surface (its bactericidal ratio was 58.7% as shown in Fig. 9), hence, backwashing with water could not recover its initial flux.

In literature, most of the previous studies evaluated the anti-biofouling property of the membranes under static conditions (no filtration applied and only static incubation with bacteria) [61–64] and only a few studies focused on the test under dynamic *E. coli* filtration conditions [25,53]. For instance, Nisola et al. [65], filtered *E. coli* solution (1×10^5 CFU/mL) through silver nanoparticle-loaded polyether-*block*-polyamide copolymer (PEBA) coated on polysulfone support. At the end of 30 h of filtration, they observed ~90% flux recovery after 5 h of washing with DI water whereas we observed ~95% flux recovery after filtering 10 times more concentrated *E. coli* solution (1×10^6 CFU/mL) and backwashing in a shorter period of time (~30 min). It should be noted that we observed a very high recovery, ~100%, even though we used a dead-end filtration unit which is known to cause a thicker bacterial cake layer formation as compared to cross flow filtration units. Based on this fact, we can expect that biofouling tendency of our membranes would be much lower if the filtration was performed in a cross-flow module. In another study, Yoosefi Booshehri et al. [31], developed regenerative coating of silver nanoparticles/multi-walled carbon nanotubes (Ag/MWNTs) on the surface of PAN hollow fiber membranes. They reported that after the filtration of ~2000 L/m^2 of bacterial solution (*E. coli* concentration of 2×10^6 CFU/mL) during 40 h, the water permeability dropped ~30% compared to the initial permeability. They reported the silver loss as 25.6% at the end of 10 h filtration (3 L of filtrate) and 56% at the end of 24 h filtration (7.2 L of

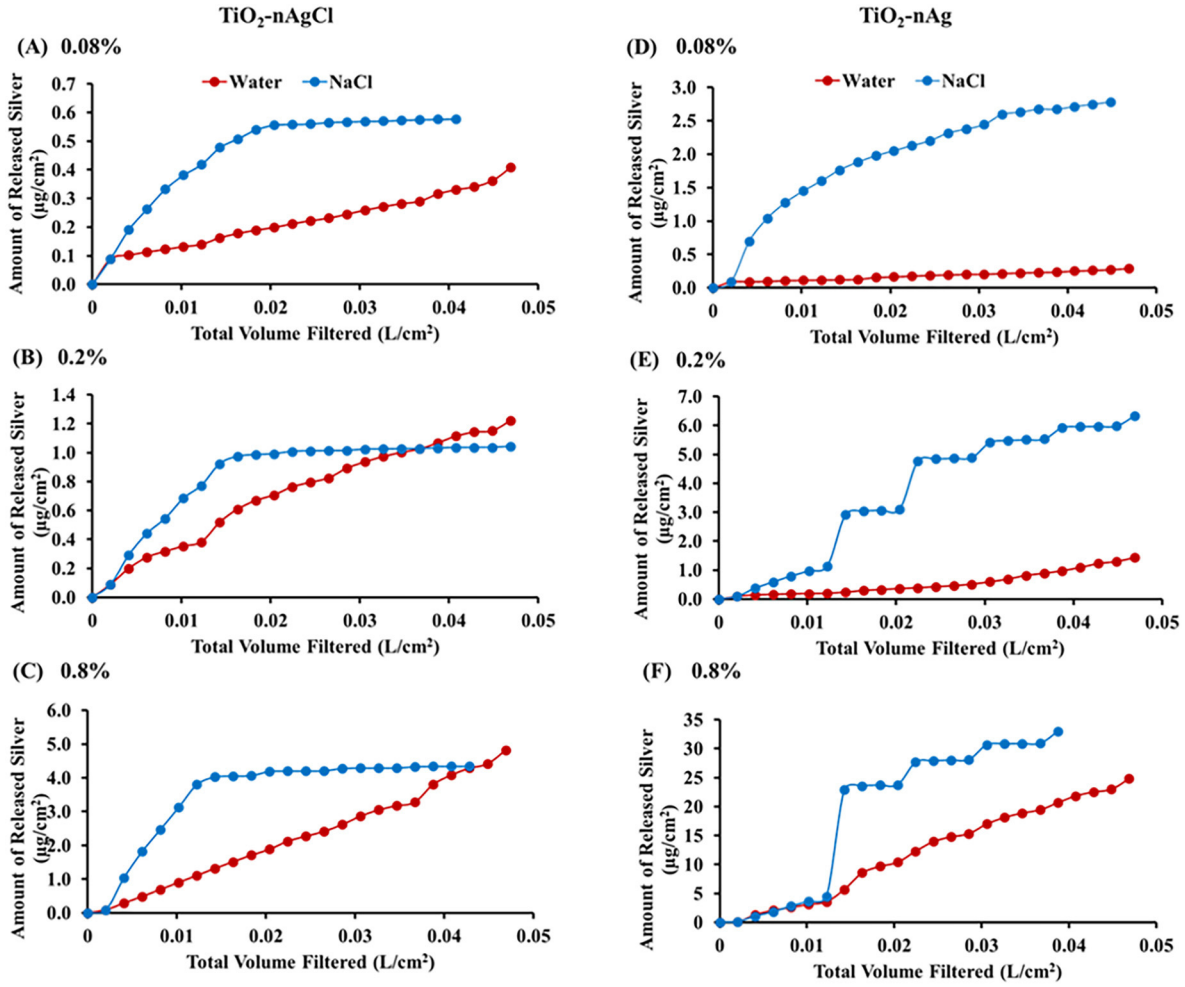

Fig. 7. Total amount of silver released from the PAN membranes containing (A) 0.08% AgCl-TiO_2 (B) 0.2% AgCl-TiO_2 (C) 0.8% AgCl-TiO_2 (D) 0.08% Ag-TiO_2 (E) 0.2% Ag-TiO_2 (F) 0.8% Ag-TiO_2 xerogels when water and 1 M NaCl solution was filtered.

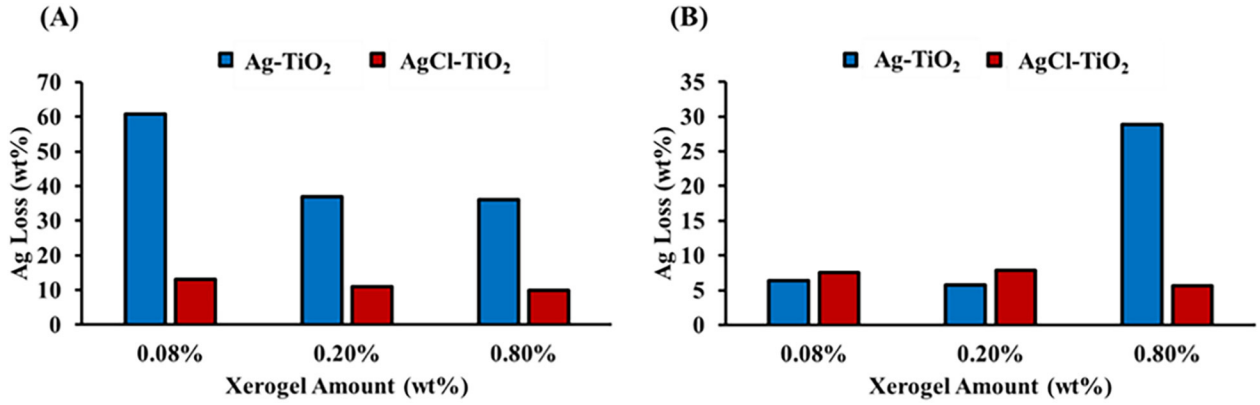

Fig. 8. Silver loss (wt%) from Ag-TiO_2 and AgCl-TiO_2 xerogels containing PAN membranes (A) when 1 M NaCl solution was filtered and (B) when water was filtered.

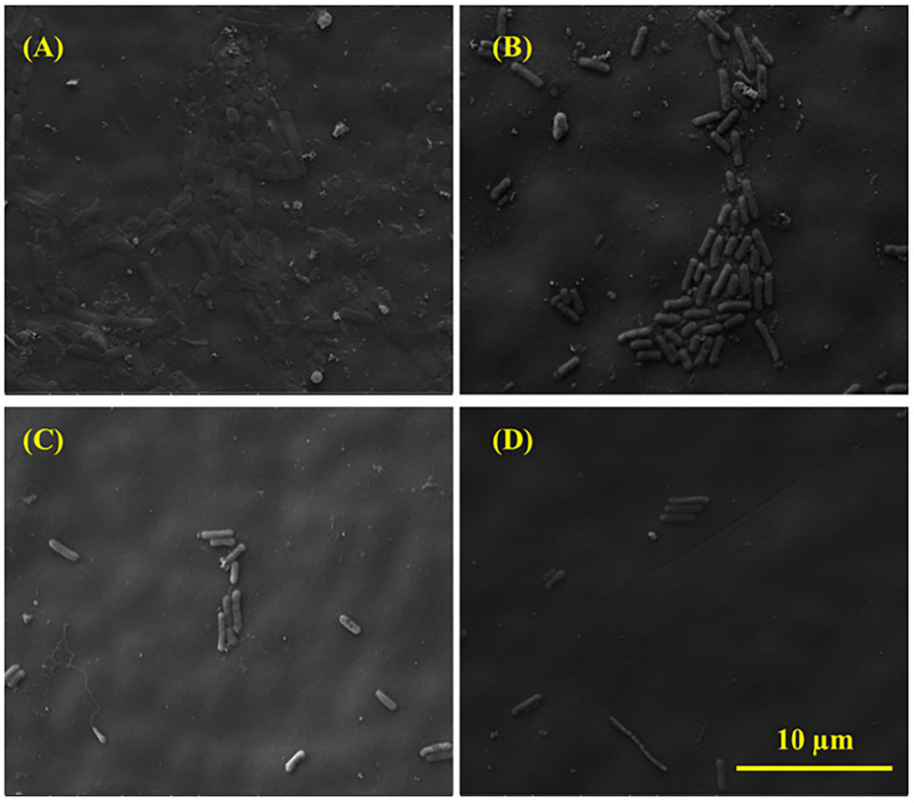

Xerogel Content in PAN Membranes (wt. %)	Surface Coverage by Bacteria (%)	Bactericidal Ratio (%)
0	80	
0.08	33	58.7
0.2	12	85
0.8	8	90

Fig. 9. SEM images of bacterial fouling on membranes (A) PAN (B) 0.08% AgCl-TiO_2 xerogels containing PAN membranes (C) 0.2% AgCl-TiO_2 xerogels containing PAN membrane (D) 0.8% AgCl-TiO_2 xerogels containing PAN membrane. Images were taken after 5 cycles of bacteria solution filtration and 3 cycles of backwash.

filtrate). Although the remaining silver within the matrix initially slowed down the bacterial growth due to very fast and high silver release, it is expected that the antibacterial effect of their membrane will be for a short period. Our results demonstrated that during the filtration of 1 M NaCl a constant silver release rate of ~2 µg/h was reached after the seventh filtration cycle for the PAN membrane containing 0.2 wt% of AgCl-TiO_2 xerogel. Based on this constant release rate (~2 µg/h), we theoretically estimated that the lifetime of an ~1 m^2 of a membrane could be 46,400 h corresponding to ~5.8 years for 8000 h of operation a year in the presence of 1 M NaCl concentration. This is the lifetime of

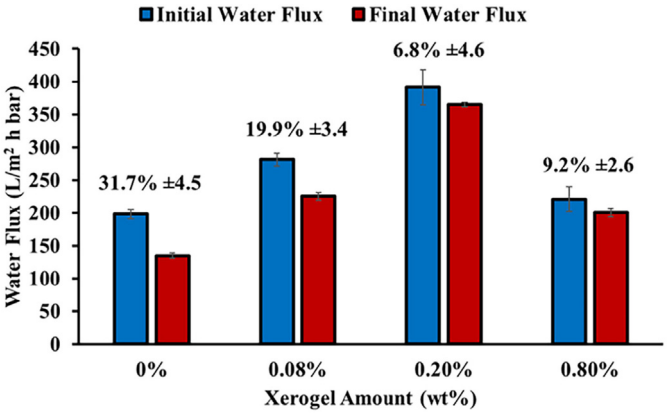

Fig. 10. Water flux before and after bacteria solution filtration and backwash cycles in PAN membranes incorporated with different amounts of AgCl-TiO_2 xerogels ($p < 0.05$). The numbers on the bars represent the percent flux decline.

0.2 wt% AgCl/TiO_2 xerogel loaded membrane where 1 m^2 of the membrane contains 92.8 mg of AgCl. Most previous studies evaluated the silver release using DI water or tap water as a release medium [23,30,35,36] or under static conditions [19,66] making it difficult to compare our results with the others. For instance, Li et al., (2019) [66] reported a 0.31% Ag^+ release per day from cellulose/silver composites and they predicted that the Ag^+ could be completely released into DI water in 323 days. The lifetime of this composite is expected to be shorter under dynamic conditions and in the presence of high salinity due to the faster release of metallic silver into NaCl than its release into DI water. This drawback has been addressed in our study by incorporating AgCl instead of Ag in the membranes. We claim that Ag could dissolve much more than AgCl in the presence of chloride ions and we have proven this hypothesis as shown by the release profiles in Fig. 7. To the best of our knowledge, no study in the literature measured the release rate under dynamic conditions using such high salinity water. Thus, a direct comparison of our lifetime estimation with other studies is not possible. The durability of our membrane in terms of its antibacterial activity will be longer if the solution contains lower NaCl concentration, such as 5.9 g/L, used in previous studies.

3.4. Long-term antibacterial activity of membranes

The antibacterial activities of the fresh and used membranes were evaluated using disk diffusion test (Fig. 11).

Both unused and used membranes incorporated with AgCl-TiO_2 xerogels showed significantly higher antibacterial activity than the membranes with Ag-TiO_2 xerogels. We found that the antibacterial activity of the membranes increased with the xerogel content. Following the 5 cycles of 1 M NaCl filtration, the AgCl-TiO_2 loaded used membranes demonstrated similar levels of antibacterial efficacy as their fresh counterparts whereas the antibacterial efficacy of the used membranes containing Ag-TiO_2 xerogels decreased. These findings can be attributed to the significantly higher silver retaining capability of the 0.2 and 0.8 wt% of AgCl-TiO_2 xerogel loaded membranes (~90% of the initial silver amount) as compared to the corresponding Ag-TiO_2 loaded membranes (~46.5% of initial silver amount) at the end of 5 filtration cycles of 1 M NaCl solution (Fig. 8A). The long term antibacterial activity of the AgCl-TiO_2 xerogels loaded PAN membranes was mainly due to the slow release rate of silver ions (Fig. 7) allowing continuously the presence of a small amount of silver in bacteria suspension (~1 μg/L, ~2.5 μg/L and ~10 μg/L for 0.08 wt%, 0.2 wt% and 0.8 wt% AgCl-TiO_2 xerogels incorporated membranes respectively). The findings in this study are also in agreement with the results reported in our previous studies indicating that the AgCl-TiO_2 xerogels, either in powder form or incorporated in membrane structures, could be used several times without losing antibacterial activity [39,41].

In the literature, there are reports on the antibacterial activity of pure TiO_2 against bacteria usually when irradiated with near-UV light. Most of the studies on TiO_2 are based on nano-TiO_2 particles which are known to be photocatalytically active in near UV to the blue region of visible light. Thus, the antibacterial mechanism on nano-TiO_2 proceeds with the formation of radicals under the near UV and/or visible light that kills bacteria [67–69]. The difference between this study and the ones in the literature is the preparation method and also we did not use UV or visible light when testing antibacterial activities of xerogel

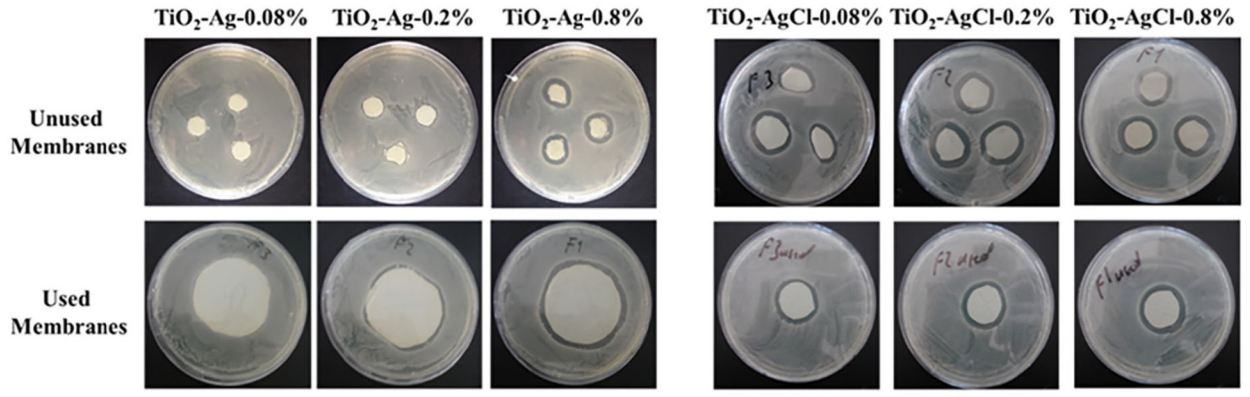

Zone Diameter (mm)						
	TiO_2-Ag-0.08%	TiO_2-Ag-0.2%	TiO_2-Ag-0.8%	TiO_2-AgCl-0.08%	TiO_2-AgCl-0.2%	TiO_2-AgCl-0.8%
Unused Membranes	0.0 ±0.0	1.0 ±0.3	4.3 ±0.3	5.1 ±0.4	7.2 ±0.3	7.3 ±0.5
Used Membranes	0.0 ±0.0	1.8 ±0.5	3.1 ±0.5	4.7 ±0.1	6.9 ±0.13	7.0 ±0.15

Fig. 11. The antibacterial activity of prepared PAN membranes incorporated with various amounts of TiO_2-nAg or TiO_2-nAgCl (0.08, 0.2 and 0.8 wt%) particles before and after 5 cycles of 1 M NaCl filtration against *E. coli* (1×10^6 CFU/mL).

incorporated PAN membranes. In our previous studies, we showed that TiO_2 xerogel without Ag or AgCl, prepared using the same procedure, did not show any bacterial activity based on the viable cell counting method [41]. Thus, the antibacterial activity reported in this study is solely due to silver ion released from AgCl/TiO_2 and Ag/TiO_2 xerogels incorporated PAN membranes.

4. Conclusion

We demonstrated that AgCl-TiO_2 xerogels in PAN membrane provided lower silver release into high-salinity water (1 M NaCl) as compared to Ag-TiO_2 in the same membrane. In addition to slow silver ion release, the AgCl-TiO_2 incorporated PAN membranes showed high water permeability, enhanced anti-biofouling, and antibacterial activity. The silver release from the 0.2% AgCl-TiO_2 in PAN membrane stayed constant at ~1 μg/cm^2 after a total filtration of 0.05 L/cm^2 1 M NaCl solution and almost 90% of the initial silver loading was retained in the membrane. Theoretical estimation suggests a potential long-term use of 5.8 years for the 0.2% AgCl-TiO_2 loaded PAN membrane even in the presence of a very high NaCl concentration. Following 5 cycles of *E. coli* solution filtration through this membrane, ~100% of water flux recovery was achieved after simple rinsing and also, antibacterial activity of used membrane did not significantly change within the experimental uncertainty of this study. The promising features of our membrane could further be tested in a larger scale cross flow filtration unit. The ease of membrane manufacturing and the ability to control the release rate of silver through adjusting the texture of AgCl-TiO_2 xerogels may have important implications for preparing novel ultrafiltration membranes with improved long-term biofouling resistance. This work could lead to the development of new silver chloride containing antibacterial membranes.

CRediT authorship contribution statement

Metin Uz: Investigation, Formal analysis, Data curation, Writing - original draft. **Filiz Yasar Mahlicli:** Formal analysis, Investigation, Methodology. **Erol Seker:** Investigation, Writing - original draft, Writing - review & editing. **Sacide Alsoy Altinkaya:** Conceptualization, Writing - original draft, Writing - review & editing, Supervision.

Declaration of competing interest

The authors declare that they have no known competing financial interests or personal relationships that could have appeared to influence the work reported in this paper.

Acknowledgment

We'd like to thank Biotechnology/Bioengineering, Environmental and Materials Research Centers at Izmir Institute of Technology for their technical support. We acknowledge Mert Tuncer for his support on the synthesis of Ag-TiO_2 and AgCl-TiO_2 xerogels.

References

[1] https://www.who.int/news-room/fact-sheets/detail/drinking-water (Last accessed: April 20, 2020).
[2] B. Alemán, W. Regan, S. Aloni, V. Altoe, N. Alem, C. Girit, B. Geng, L. Maserati, M. Crommie, F. Wang, A. Zettl, Transfer-free batch fabrication of large-area suspended graphene membranes, ACS Nano 4 (2010) 4762–4768.
[3] L. Qi, Z. Xu, X. Jiang, C. Hu, X. Zou, Preparation and antibacterial activity of chitosan nanoparticles, Carbohydr. Res. 339 (2004) 2693–2700.
[4] J.R. Morones, J.L. Elechiguerra, A. Camacho, K. Holt, J.B. Kouri, J.T. Ramirez, M.J. Yacaman, The bactericidal effect of silver nanoparticles, Nanotechnology 16 (2005) 2346–2353.
[5] C. Wei, W.Y. Lin, Z. Zainal, N.E. Williams, K. Zhu, A.P. Kruzic, R.L. Smith, K. Rajeshwar, Bactericidal activity of TiO2 photocatalyst in aqueous media: toward a solar-assisted water disinfection system, Environ. Sci. Technol. 28 (1994) 934–938.
[6] M. Cho, H. Chung, W. Choi, J. Yoon, Different Inactivation Behaviors of MS-2 Phage and *Escherichia coli* in TiO_2 Photocatalytic Disinfection, Appl. Environ. Microbiol. 71 (2005) 270.
[7] A.R. Badireddy, E.M. Hotze, S. Chellam, P. Alvarez, M.R. Wiesner, Inactivation of bacteriophages via photosensitization of fullerol nanoparticles, Environ. Sci. Technol. 41 (2007) 6627–6632.
[8] D.Y. Lyon, L.K. Adams, J.C. Falkner, P.J.J. Alvarez, Antibacterial activity of fullerene water suspensions: effects of preparation method and particle size, Environ. Sci. Technol. 40 (2006) 4360–4366.
[9] S. Kang, M. Pinault, L.D. Pfefferle, M. Elimelech, Single-walled carbon nanotubes exhibit strong antimicrobial activity, Langmuir 23 (2007) 8670–8673.
[10] Y. Zhang, Y. Chen, P. Westerhoff, K. Hristovski, J.C. Crittenden, Stability of commercial metal oxide nanoparticles in water, Water Res. 42 (2008) 2204–2212.
[11] C.P. Tso, C.M. Zhung, Y.H. Shih, Y.M. Tseng, S.C. Wu, R.A. Doong, Stability of metal oxide nanoparticles in aqueous solutions, Water Sci. Technol. J. Int. Assoc. Water Pollut. Res. 61 (2010) 127–133.
[12] B. Meyer, Approaches to prevention, removal and killing of biofilms, Int. Biodeterior. Biodegradation 51 (2003) 249–253.
[13] M.M. Pendergast, E.M.V. Hoek, A review of water treatment membrane nanotechnologies, Energy Environ. Sci. 4 (2011) 1946–1971.
[14] J.J. Harrison, H. Ceri, C.A. Stremick, R.J. Turner, Biofilm susceptibility to metal toxicity, Environ. Microbiol. 6 (2004) 1220–1227.
[15] E.-S. Kim, G. Hwang, M. Gamal El-Din, Y. Liu, Development of nanosilver and multi-walled carbon nanotubes thin-film nanocomposite membrane for enhanced water treatment, J. Membr. Sci. 394–395 (2012) 37–48.
[16] S. Liu, M. Zhang, F. Fang, L. Cui, J. Wu, R. Field, K. Zhang, Biogenic silver nanocomposite TFC nanofiltration membrane with antifouling properties, Desalin. Water Treat. 57 (2016) 10560–10571.
[17] M.C. Cruz, G. Ruano, M. Wolf, D. Hecker, E. Castro Vidaurre, R. Schmittgens, V.B. Rajal, Plasma deposition of silver nanoparticles on ultrafiltration membranes: antibacterial and anti-biofouling properties, Chem. Eng. Res. Des. 94 (2015) 524–537.
[18] F. Diagne, R. Malaisamy, V. Boddie, R.D. Holbrook, B. Eribo, K.L. Jones, Polyelectrolyte and silver nanoparticle modification of microfiltration membranes to mitigate organic and bacterial fouling, Environ. Sci. Technol. 46 (2012) 4025–4033.
[19] M.S. Haider, G.N. Shao, S.M. Imran, S.S. Park, N. Abbas, M.S. Tahir, M. Hussain, W. Bae, H.T. Kim, Aminated polyethersulfone-silver nanoparticles (AgNPs-APES) composite membranes with controlled silver ion release for antibacterial and water treatment applications, Mater. Sci. Eng. C Mater. Biol. Appl. 62 (2016) 732–745.
[20] S. Kawada, D. Saeki, H. Matsuyama, Development of ultrafiltration membrane by stacking of silver nanoparticles stabilized with oppositely charged polyelectrolytes, Colloids Surf. A Physicochem. Eng. Asp. 451 (2014) 33–37.
[21] J.-H. Li, X.-S. Shao, Q. Zhou, M.-Z. Li, Q.-Q. Zhang, The double effects of silver nanoparticles on the PVDF membrane: surface hydrophilicity and antifouling performance, Appl. Surf. Sci. 265 (2013) 663–670.
[22] Q. Liu, Z. Zhou, G. Qiu, J. Li, J. Xie, J.Y. Lee, Surface reaction route to increase the loading of antimicrobial Ag nanoparticles in forward osmosis membranes, ACS Sustain. Chem. Eng. 3 (2015) 2959–2966.
[23] S. Liu, F. Fang, J. Wu, K. Zhang, The anti-biofouling properties of thin-film composite nanofiltration membranes grafted with biogenic silver nanoparticles, Desalination 375 (2015) 121–128.
[24] M.S. Mauter, Y. Wang, K.C. Okemgbo, C.O. Osuji, E.P. Giannelis, M. Elimelech, Antifouling ultrafiltration membranes via post-fabrication grafting of biocidal nanomaterials, ACS Appl. Mater. Interfaces 3 (2011) 2861–2868.
[25] S.-H. Park, S.H. Kim, S.-J. Park, S. Ryoo, K. Woo, J.S. Lee, T.-S. Kim, H.-D. Park, H. Park, Y.-I. Park, J. Cho, J.-H. Lee, Direct incorporation of silver nanoparticles onto thin-film composite membranes via arc plasma deposition for enhanced antibacterial and permeation performance, J. Membr. Sci. 513 (2016) 226–235.
[26] I. Sawada, R. Fachrul, T. Ito, Y. Ohmukai, T. Maruyama, H. Matsuyama, Development of a hydrophilic polymer membrane containing silver nanoparticles with both organic antifouling and antibacterial properties, J. Membr. Sci. 387–388 (2012) 1–6.
[27] L. Tang, K.A. Huynh, M.L. Fleming, M. Larronde-Larretche, K.L. Chen, Imparting antimicrobial and anti-adhesive properties to polysulfone membranes through modification with silver nanoparticles and polyelectrolyte multilayers, J. Colloid Interface Sci. 451 (2015) 125–133.
[28] M. Toroghi, A. Raisi, A. Aroujalian, Preparation and characterization of polyethersulfone/silver nanocomposite ultrafiltration membrane for antibacterial applications, Polym. Adv. Technol. 25 (2014) 711–722.
[29] E. Yang, K.-J. Chae, A.B. Alayande, K.-Y. Kim, I.S. Kim, Concurrent performance improvement and biofouling mitigation in osmotic microbial fuel cells using a silver nanoparticle-polydopamine coated forward osmosis membrane, J. Membr. Sci. 513 (2016) 217–225.
[30] J. Yin, Y. Yang, Z. Hu, B. Deng, Attachment of silver nanoparticles (AgNPs) onto thin-film composite (TFC) membranes through covalent bonding to reduce membrane biofouling, J. Membr. Sci. 441 (2013) 73–82.
[31] A. Yoosefi Booshehri, R. Wang, R. Xu, The effect of re-generable silver nanoparticles/multi-walled carbon nanotubes coating on the antibacterial performance of hollow fiber membrane, Chem. Eng. J. 230 (2013) 251–259.
[32] S. Zhang, G. Qiu, Y.P. Ting, T.-S. Chung, Silver–PEGylated dendrimer nanocomposite coating for anti-fouling thin film composite membranes for water treatment, Colloids Surf. A Physicochem. Eng. Asp. 436 (2013) 207–214.
[33] Y. Zhang, Y. Wan, Y. Shi, G. Pan, H. Yan, J. Xu, M. Guo, L. Qin, Y. Liu, Facile modification of thin-film composite nanofiltration membrane with silver

nanoparticles for anti-biofouling, J. Polym. Res. 23 (2016) 105.
[34] A. Alpatova, E.-S. Kim, X. Sun, G. Hwang, Y. Liu, M. Gamal El-Din, Fabrication of porous polymeric nanocomposite membranes with enhanced anti-fouling properties: effect of casting composition, J. Membr. Sci. 444 (2013) 449–460.
[35] J. Huang, H. Wang, K. Zhang, Modification of PES membrane with Ag–SiO2: reduction of biofouling and improvement of filtration performance, Desalination 336 (2014) 8–17.
[36] X. Li, R. Pang, J. Li, X. Sun, J. Shen, W. Han, L. Wang, In situ formation of Ag nanoparticles in PVDF ultrafiltration membrane to mitigate organic and bacterial fouling, Desalination 324 (2013) 48–56.
[37] K. Zodrow, L. Brunet, S. Mahendra, D. Li, A. Zhang, Q. Li, P.J.J. Alvarez, Polysulfone ultrafiltration membranes impregnated with silver nanoparticles show improved biofouling resistance and virus removal, Water Res. 43 (2009) 715–723.
[38] D. Qadir, H. Mukhtar, L.K. Keong, Mixed matrix membranes for water purification applications, Sep. Purif. Rev. 46 (2017) 62–80.
[39] P. Kaner, D.J. Johnson, E. Seker, N. Hilal, S.A. Altinkaya, Layer-by-layer surface modification of polyethersulfone membranes using polyelectrolytes and AgCl/TiO2 xerogels, J. Membr. Sci. 493 (2015) 807–819.
[40] C. Glass, J. Silverstein, Denitrification of high-nitrate, high-salinity wastewater, Water Res. 33 (1999) 223–229.
[41] M. Tuncer, E. Seker, Single step sol-gel made silver chloride on Titania xerogels to inhibit *E. coli* bacteria growth: effect of preparation and chloride ion on bactericidal activity, J. Sol-Gel Sci. Technol. 59 (2011) 304–310.
[42] H. Karkhanechi, R. Takagi, H. Matsuyama, Biofouling resistance of reverse osmosis membrane modified with polydopamine, Desalination 336 (2014) 87–96.
[43] J. Buckman, A.S. Bankole, S. Zihms, H. Lewis, G. Couples, W.P. Corbett, Quantifying porosity through automated image collection and batch image processing: case study of three carbonates and an aragonite cemented sandstone, Geosciences 7 (2017).
[44] A.K. Hołda, I.F.J. Vankelecom, Understanding and guiding the phase inversion process for synthesis of solvent resistant nanofiltration membranes, J. Appl. Polym. Sci. (2015) 132 (n/a-n/a).
[45] Y. Pan, Preparation and Characterization of Membranes Formed by Nonsolvent Induced Phase Separation: A Review, (2010).
[46] J.-F. Li, Z.-L. Xu, H. Yang, L.-Y. Yu, M. Liu, Effect of TiO2 nanoparticles on the surface morphology and performance of microporous PES membrane, Appl. Surf. Sci. 255 (2009) 4725–4732.
[47] W.Y. Gan, S.W. Lam, K. Chiang, R. Amal, H. Zhao, M.P. Brungs, Novel TiO2 thin film with non-UV activated superwetting and antifogging behaviours, J. Mater. Chem. 17 (2007) 952–954.
[48] R. Wang, K. Hashimoto, A. Fujishima, M. Chikuni, E. Kojima, A. Kitamura, M. Shimohigoshi, T. Watanabe, Light-induced amphiphilic surfaces, Nature 388 (1997) 431.
[49] R. Wang, K. Hashimoto, A. Fujishima, M. Chikuni, E. Kojima, A. Kitamura, M. Shimohigoshi, T. Watanabe, Photogeneration of highly amphiphilic TiO2 surfaces, Adv. Mater. 10 (1998) 135–138.
[50] Y. Wang, Q. Yang, G. Shan, C. Wang, J. Du, S. Wang, Y. Li, X. Chen, X. Jing, Y. Wei, Preparation of silver nanoparticles dispersed in polyacrylonitrile nanofiber film spun by electrospinning, Mater. Lett. 59 (2005) 3046–3049.
[51] D. Kharaghani, M.Q. Khan, A. Shahrzad, Y. Inoue, T. Yamamoto, S. Rozet, Y. Tamada, I.S. Kim, Preparation and in-vitro assessment of hierarchal organized antibacterial breath mask based on polyacrylonitrile/silver (PAN/AgNPs) nanofiber, Nanomaterials (Basel, Switzerland) (2018) 8.
[52] M. Cheryan, Ultrafiltration and Microfiltration Handbook, Taylor & Francis, 1998.
[53] Z.M. Xiu, Q.B. Zhang, H.L. Puppala, V.L. Colvin, P.J. Alvarez, Negligible particle-specific antibacterial activity of silver nanoparticles, Nano Lett. 12 (2012) 4271–4275.
[54] C. Levard, S. Mitra, T. Yang, A.D. Jew, A.R. Badireddy, G.V. Lowry, G.E. Brown, Effect of chloride on the dissolution rate of silver nanoparticles and toxicity to *E. coli*, Environ. Sci. Technol. 47 (2013) 5738–5745.
[55] Knovel Critical Tables (2nd edition).Knovel Corporation. https://app.knovel.com/web/toc.v/cid:kpKCTE000X/viewerType:toc/. Last accessed: April 20, 2020. Copyright Date: 2008, ISBNN/AEl ectronic, ISBN 978-1-59124-550-6. Knovel Release Date: 2003-02-01.
[56] T.M. Seward, The stability of chloride complexes of silver in hydrothermal solutions up to 350°C, Geochim. Cosmochim. Acta 40 (1976) 1329–1341.
[57] D. Kostic, S. Vidovic, B. Obradovic, Silver release from nanocomposite Ag/alginate hydrogels in the presence of chloride ions: experimental results and mathematical modeling, J. Nanopart. Res. 18 (2016) 76.
[58] T.A. Dankovich, Microwave-assisted incorporation of silver nanoparticles in paper for point-of-use water purification, Environ. Sci. Nano 1 (2014) 367–378.
[59] A. Subramani, E.M.V. Hoek, Direct observation of initial microbial deposition onto reverse osmosis and nanofiltration membranes, J. Membr. Sci. 319 (2008) 111–125.
[60] L.C. Gomes, L.N. Silva, M. Simões, L.F. Melo, F.J. Mergulhão, *Escherichia coli* adhesion, biofilm development and antibiotic susceptibility on biomedical materials, J. Biomed. Mater. Res. A 103 (2015) 1414–1423.
[61] P.F. Andrade, A.F. de Faria, F.J. Quites, S.R. Oliveira, O.L. Alves, M.A.Z. Arruda, M.D. Goncalves, Inhibition of bacterial adhesion on cellulose acetate membranes containing silver nanoparticles, Cellulose 22 (2015) 3895–3906.
[62] L.F. Villalobos, S. Chisca, H. Cheng, P.-Y. Hong, S. Nunes, K.-V. Peinemann, In situ growth of biocidal AgCl crystals in the top layer of asymmetric polytriazole membranes, RSC Adv. 6 (2016) 46696–46701.
[63] J.Y. Zhang, Y.T. Zhang, Y.F. Chen, L. Du, B. Zhang, H.Q. Zhang, J.D. Liu, K.J. Wang, Preparation and characterization of novel polyethersulfone hybrid ultrafiltration membranes bending with modified halloysite nanotubes loaded with silver nanoparticles, Ind. Eng. Chem. Res. 51 (2012) 3081–3090.
[64] Y. Jiang, D. Liu, M.J. Cho, S.S. Lee, F.Z. Zhang, P. Biswas, J.D. Fortner, In situ photocatalytic synthesis of Ag nanoparticles (nAg) by crumpled graphene oxide composite membranes for filtration and disinfection applications, Environ. Sci. Technol. 50 (2016) 2514–2521.
[65] G.M. Nisola, J.S. Park, A.B. Beltran, W.J. Chung, Silver nanoparticles in a polyether-block-polyamide copolymer towards antimicrobial and antifouling membranes, RSC Adv. 2 (2012) 2439–2448.
[66] J. Li, L. Kang, B. Wang, K. Chen, X. Tian, Z. Ge, J. Zeng, J. Xu, W. Gao, Controlled release and long-term antibacterial activity of dialdehyde nanofibrillated cellulose/silver nanoparticle composites, ACS Sustain. Chem. Eng. 7 (2019) 1146–1158.
[67] H.J. Haugen, S.P. Lyngstadaas, M.S. Ågren (Ed.), Wound Healing Biomaterials, Woodhead Publishing, 2016, pp. 439–450.
[68] P.C. Maness, S. Smolinski, D.M. Blake, Z. Huang, E.J. Wolfrum, W.A. Jacoby, Bactericidal activity of photocatalytic TiO(2) reaction: toward an understanding of its killing mechanism, Appl. Environ. Microbiol. 65 (1999) 4094–4098.
[69] Y. Gao, Y. Han, M. Cui, H.L. Tey, L. Wang, C. Xu, ZnO nanoparticles as an antimicrobial tissue adhesive for skin wound closure, J. Mater. Chem. B 5 (2017) 4535–4541.